MedChemComm

RESEARCH ARTICLE

View Article Online
View Journal | View Issue

Cite this: *Med. Chem. Commun.*, 2018, **9**, 2045

Exploring the effectiveness of novel benzimidazoles as CB2 ligands: synthesis, biological evaluation, molecular docking studies and ADMET prediction†

Michele Tonelli, *[a] Elena Cichero,[a] Alì Mokhtar Mahmoud,[b] Alessandro Rabbito,[b] Bruno Tasso,[a] Paola Fossa‡[a] and Alessia Ligresti‡[b]

Received 12th September 2018,
Accepted 7th October 2018

DOI: 10.1039/c8md00461g

rsc.li/medchemcomm

Herein we continued our previous work on the development of CB2 ligands, reporting the design and synthesis of a series of benzimidazole-containing derivatives that were explored as selective CB2 ligands with binding affinity towards both CB1 and CB2 receptors. Seven out of eighteen compounds exhibited preferential binding ability to CB2 over CB1 receptors with potencies in the sub-micromolar or low micromolar range. In particular, we identified two promising hit compounds, the agonist 1-[2-(*N*,*N*-diethylamino)ethyl]-2-(4-ethoxybenzyl)-5-trifluoromethylbenzimidazole (**3**) (CB2: K_i = 0.42 μM) and the inverse agonist/antagonist 1-butyl-2-(3,4-dichlorobenzyl)-5-trifluoromethylbenzimidazole (**11**) (CB2: K_i = 0.37 μM). Docking studies also performed on other benzimidazoles reported in the literature supported the structure–activity relationship observed in this series of compounds and allowed the key contacts involved in the agonist and/or inverse agonist behaviour displayed by these derivatives to be determined. The *in silico* evaluation of ADMET properties suggested a favorable pharmacokinetic and safety profile, promoting the drug-likeness of these compounds towards a further optimization process.

Introduction

Endocannabinoids and their receptors (CB1 and CB2) constitute a large modulatory system that finely tunes the synaptic neurotransmission and consequently a complex network of physiological and pathological processes.[1,2]

The CB1 and CB2 cannabinoid receptors are G-protein coupled receptors (GPCRs), which primarily couple with the G proteins of the G_i and G_o classes.[3] Receptor activation inhibits adenylyl cyclases and certain voltage-dependent calcium channels as well as activates several mitogen-activated protein kinases and inwardly rectifies potassium channels, with some variation depending on the particular cell type.[3] Activation of CB1 or CB2 receptors controls the cannabinoid signal transduction pathways at different levels, exerting diverse consequences on cellular physiology, including synaptic function, gene transcription, and cell motility.

CB1 is widely expressed within the central nervous system (CNS),[4] where it mediates the psychotropic effects of (−)-*trans*-Δ9-tetrahydrocannabinol (THC).[5]

The failure of the CB1 receptor inverse agonist rimonabant in 2009 (ref. 6) motivated researchers to explore more deeply the presence and function of this receptor in peripheral non-neuronal tissues (adipose tissue, liver, gastrointestinal tract, pancreas, and skeletal muscles). Accordingly, peripherally-restricted CB1 receptor antagonists/inverse agonists have been shown to effectively reduce body weight, adiposity, insulin resistance and dyslipidaemia in obese animal models.[7]

This widely distributed and differential expression of CB1 receptors both in the brain and in the periphery reflects the complexity and can justify the variety of functions of endocannabinoids.[8]

CB2 receptors are expressed at much lower levels in the CNS compared to CB1 receptors. These receptors are predominantly located in immune cells, although recent studies have found the expression of genes that encode this receptor even in the cerebellum[9] and in microglia.[10]

Based on the ability of WIN-55,212-2 to activate unselectively CB1 as well as CB2 subtypes, numerous studies arose with the aim of designing a new series of analogues with better selectivity and potency profiles towards the

[a] *Dipartimento di Farmacia, Università degli Studi di Genova, V.le Benedetto XV, 3, 16132 Genova, Italy. E-mail: tonelli@difar.unige.it*
[b] *National Research Council of Italy, Institute of Biomolecular Chemistry, Endocannabinoid Research Group, Via Campi Flegrei 34, 80078 Pozzuoli, (Na), Italy*

† Electronic supplementary information (ESI) available: Table 1S and ^{1}H and ^{13}C NMR spectra of compound **14** are reported. See DOI: 10.1039/c8md00461g

‡ Last authors.

single CB2 receptor. Initially, research efforts were focused on the indole scaffold, derived from the molecular simplification of the reference compound WIN-55,212-2, leading to aminoalkylindoles (AAIs), such as AM630 (Fig. 1, **B**). These were considered as intriguing CB2 agonists confirming the effectiveness of replacing the WIN-55,212-2 tricyclic system with an indole core or, where appropriate, with other series of heteroaromatic systems.

This motivated the researchers to discover many interesting chemo-types, some of them still revolving around the indole structure, while the other ones are characterized by different rings, allowing the evaluation of the reliability of the bioisosteric approach.

Among the indole-based derivatives, a new series of compounds were obtained by replacing the morpholine ring of WIN-55,212-2 with a pyran one, and the 1-naphthyl residue with a tetramethylcyclopropyl substituent (Fig. 2, **C**).

These indolyl-ketones exhibited potent and selective agonist activity at the CB2 receptor,[11] even surpassing the binding affinity for the same receptor of WIN-55,212-2. The subnanomolar K_i values of this pool of molecules **1a–13a** (Fig. 2, **C**) revealed the effectiveness of non-basic substituents linked to position 1 of the indole core, as shown by the methylpyran moiety of **C** *versus* the basic ethylmorpholine chain of WIN-55,212-2. Notably, this proved to be true, independent of the nature of substituents decorating the indole ring. Concerning this issue, electron-donor groups examined in positions 6 and 7 of the indole ring were able to enhance the potency towards the CB2 receptor, (**12a**, R = 6-OCH_3: CB2 K_i = 0.51 nM, CB1 K_i = 40 nM; **13a**, R = 7-OCH_3: CB2 K_i = 0.12 nM, CB1 K_i = 45 nM), leaving the low selectivity ratio unaltered. In contrast, the substitutions with electron-withdrawing groups (F, Cl and Br) in position 5 improved the selectivity profile towards the CB2 receptor, ranging from 172 to 756. The same behavior was also maintained within those analogues featuring in position 1 the ethylmorpholine chain of the prototype (Fig. 2, **D**). Conversely, substitutions at position 4 or 7 of the indole ring were detrimental when compared with any variation involving position 2, which allowed compounds with a better profile of both affinity and selectivity towards the CB2 receptor (**19a**, R = 2-CH_3: CB2 K_i = 27 nM,

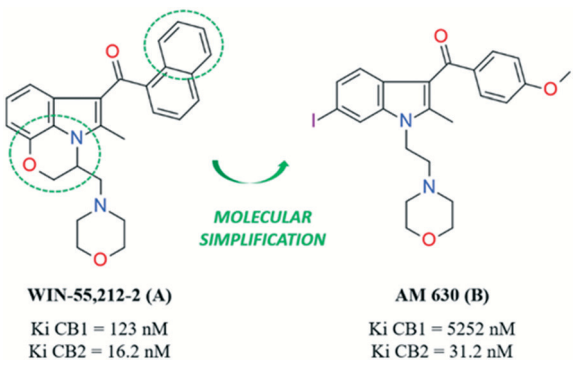

Fig. 1 Chemical structures and binding affinity values of the agonist WIN-55,212-2 and the inverse agonist/antagonist AM630.

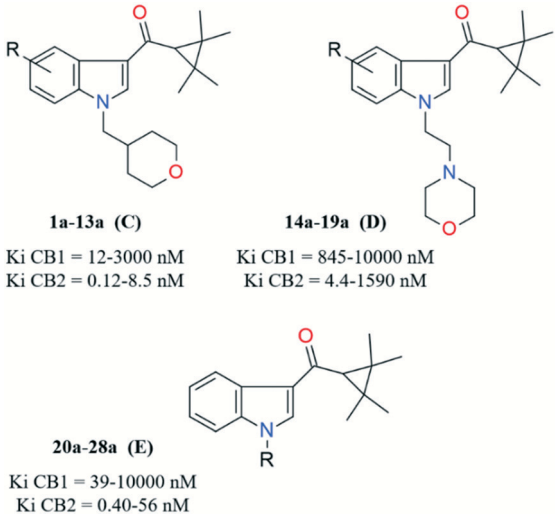

Fig. 2 Chemical structures and binding affinity values of known CB1/CB2 indole-containing agonists.

CB1 K_i > 10 000 nM) to be obtained. Starting from the aforementioned indolyl-ketones, new different chains (Fig. 2, **E**) were further explored, sometimes also varying the ketone group in position 3 with other cycloaliphatic systems, leaving the other ring positions unchanged.[12] All the investigated alcoholic or (thio)ethereal chains were characterized by suitable potency towards the CB2 receptor, in addition to a high selectivity profile. The best requirement for an improved selectivity index (SI) towards the CB2 receptor over CB1 was a linker of two carbon atoms between the indole nitrogen and an amino function (R = $(CH_2)_2N(CH_3)_2$, SI > 5263); in contrast, the introduction of a longer alkyl spacer, moving from the hydroxyethyl chain to the hydroxybutyl ones, was responsible for a higher affinity for the CB2 receptor (R = $(CH_2)_2OH$, SI > 179; $(CH_2)_3OH$, SI = 1047; $(CH_2)_4OH$, SI = 2545). It is worth noting that the absence of a basic head group in R to mimic the morpholine ring of WIN-55,212-2, in favor of a thioethereal or a carbonyl function, had however led to powerful CB2 agonists (R = $(CH_2)_4SCH_3$, CB2: K_i 0.40 nM; $(CH_2)_4COCH_3$, CB2: K_i = 0.99 nM), even if with a reduced selectivity *versus* the CB1 receptor.

While maintaining the indole core allowed so far the design of potent CB2 agonists, the search for other heterocyclic rings allowed the discovery of a series of congeners featuring agonist as well as inverse agonist activity, on the basis of specific substituents. This trend was previously observed in a series of isatin acylhydrazones discussed in the literature,[13,14] and in benzimidazole skeletons proposed by AstraZeneca[15,16] still exhibiting more potent and selective profiles towards the human CB2 receptor in comparison with WIN-55,212-2.

In particular, among the benzimidazole derivatives, it is possible to distinguish some structural features like an amide function in position 5 and a bulky lipophilic chain in position 1 (Fig. 3), associated with a valuable CB2 agonist profile, as shown by the most potent and selective compound with R = cyclobutylmethyl (CB2 = 1.6 nM, SI = 1947).[16] In

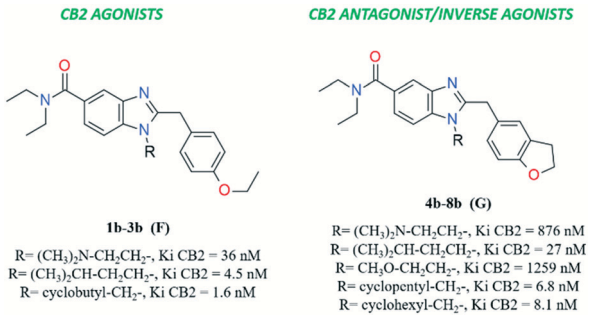

Fig. 3 Chemical structures and binding affinity values of CB2 benzimidazole-containing agonists and antagonists.

particular, the 4-ethoxybenzyl moiety was considered as the main determinant for the agonist activity of this class of compounds, independent of the nature of the chains in position 1 of the benzimidazole nucleus.

Moreover, Pagé *et al.*[17] observed that the replacement of the 4-ethoxyphenyl ring with a benzofuran one shifted the agonist profile in favor of an antagonist/inverse agonist behavior. In this set of antagonists, the authors observed that the introduction of polar atoms (N, O) in the side chain (R) matched negatively with the affinity towards the CB2 receptor, while much better results were obtained with lipophilic substitutions, particularly with alicyclic ones (R = cyclopentylmethyl and cyclohexylmethyl).

During the last few years, our research group developed a large variety of benzimidazole derivatives with different pharmacological aims, in particular, exploring the analgesic,[18] antiviral[19–21] and anti-tumor[22] activities. Our benzimidazoles, studied *in vivo* as analgesic drugs, were designed on the basis of previous work of CIBA (now Novartis), that led to etonitazene, the most potent μ-opioid currently known.[23] Besides the analgesic activity, some members of our benzimidazole sets displayed CNS stimulant, anti-inflammatory and hypotensive activities which are related to the involvement of other non-opioid receptors, eventually also the cannabinoid ones.

Based on the information coming from preliminary computational studies performed on the in-house available CB2 receptor model,[24] we *in silico* screened a series of benzimidazole-containing derivatives in order to better investigate the effect of unexplored substitutions at this core in terms of their selectivity and functionality to the CB2 receptor.

Results and discussion

Chemistry

Compounds **1–18** (Fig. 4) were re-synthesized, with the exception of the newly synthesized derivative **14**, to be evaluated as novel CB1 and CB2 ligands, bearing in positions 1, 2 and 5 of the benzimidazole core some new unexplored substitutions.

For compounds **1–2**, **5** and **6**,[25] **3**,[26] **4**, **11** and **12**,[21] and **7–10**,[27] the benzimidazole ring was formed by heating, in chloroform solution, the properly substituted 1,2-phenylenediamine with the hydrochloride of the iminoester, previously prepared from the corresponding nitrile, absolute

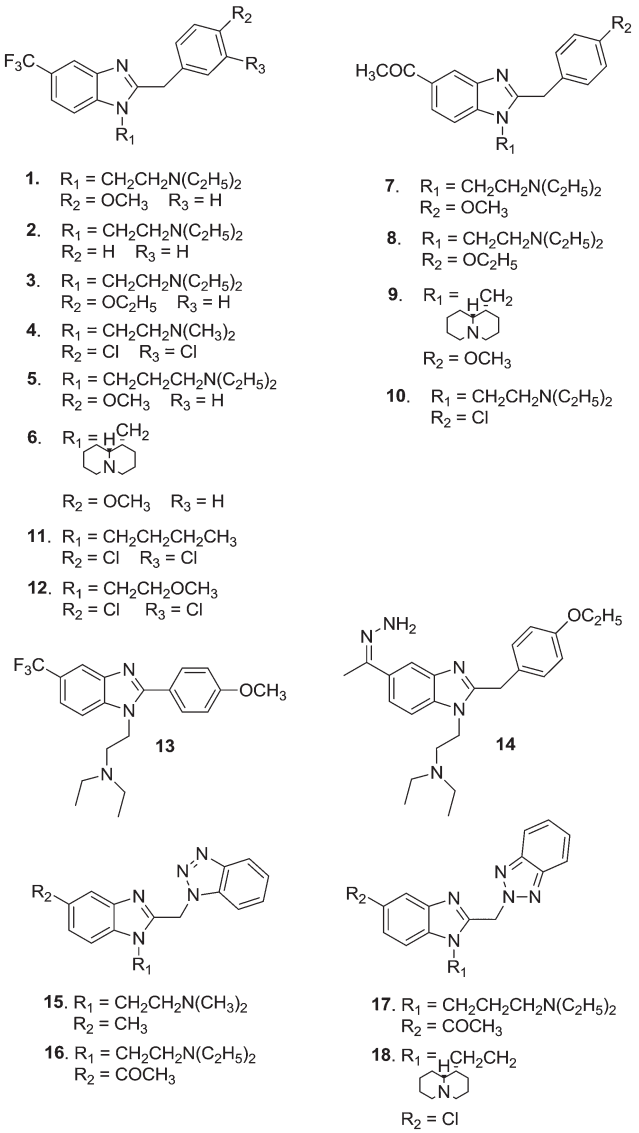

Fig. 4 Chemical structure of the investigated benzimidazole derivatives.

ethanol and dry HCl. Compound **13** was obtained by condensing *N*,*N*-diethylaminoethyl-5-trifluoromethyl-1,2-phenylenediamine with the aldehyde-sodium bisulphite adduct, which was freshly prepared, as indicated by Shriner and Land.[28] Finally, the 2-[(benzotriazol-1/2-yl)methyl]-benzimidazoles **15**,[29] **16**, **17** (ref. 30) and **18** (ref. 19) were synthesized by fusing at 180 °C a mixture of the properly substituted 1,2-phenylenediamine and (benzotriazol-1/2-yl)acetic acid.

The hydrazone derivative **14** was obtained by refluxing for 5 h a hydroalcoholic solution of 5-acetyl-1-(2-diethylaminoethyl)-2-(4-ethoxybenzyl)benzimidazole (**8**) with a slight excess of hydrazine hydrate (Scheme 1).

In vitro pharmacology and SAR

The investigated compounds (**1–18**) were evaluated using radioligand binding assays for their ability to displace [^{3}H]-

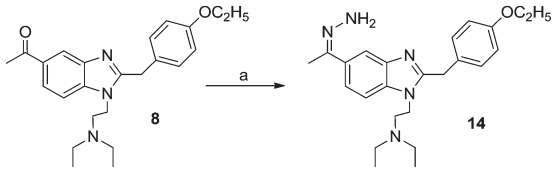

Scheme 1 Reagents and conditions: a) EtOH/H_2O, $NH_2NH_2{\cdot}H_2O$ (1.15 equiv.), 120 °C, 5 h.

CP-55,940 from human recombinant CB1 and CB2 receptors (Perkin Elmer, Italy). In Table 1, the inhibition constants (K_i) of compounds **1–18** towards the CB1 and CB2 receptors are reported. The selectivity index (SI) of CB2 *versus* CB1 is determined by dividing the CB1 K_i value by the CB2 K_i value.

The most interesting compounds showed selective binding affinity towards the CB2 receptor with K_i values ranging from 0.37 to 10 μM. Only compound **11**, the most potent CB2 ligand (K_i = 0.37 μM), was also able to bind the CB1 receptor with lower affinity, although exhibiting a preferential selectivity (SI = 27.03) for CB2 over CB1.

In comparison with previously investigated benzimidazole derivatives by Pagé *et al.* (Fig. 3),[15–17] in some cases, our compounds have the same pattern of substitutions (such as the dimethylamino and methoxyethyl chains in position 1 and the 4-ethoxyethylbenyl ring in position 2), although associating them with different decorations in positions 1, 2 and 5 of the benzimidazole core. The synthesized structures were designed by decorating the benzimidazole scaffold with substituents of different nature: a) an aliphatic chain in position 1 (basic or neutral); b) an aromatic (phenyl, benzyl) or heteroaromatic ring in position 2; c) an electron-withdrawing (CF_3, Cl, $COCH_3$) or electron-donor (CH_3, OCH_3) group in position 5. The more recurring features responsible for CB2 receptor affinity were a dialkylaminoethyl chain in position 1, a benzyl ring in position 2 and a CF_3 group in position 5 of the benzimidazole scaffold.

The structure–activity relationship study showed that the dimethylaminoethyl or diethylaminoethyl chains were best suited for promoting the binding to the CB2 receptor (**1–4**, **8**), while the longer diethylaminopropyl or the bulkier quinolizidine moieties (**6**, **9** and **18**) caused the loss of affinity. Also, neutral chains proved to be favorable for substitutions: the lipophilic *n*-butyl chain made compound **11** more effective than the analog **10**, which bears a dimethylaminoethyl chain. Indeed, compound **11** was found to be the most potent CB2 ligand, exhibiting the highest affinity value for the target (K_i = 0.37 μM); also the polar methoxyethyl chain, exhibited by **12**, was proven effective, but with a 30-fold lower affinity compared to **11**.

With regard to the substitution in position 2, the more flexible benzyl ring proved to be the only effective aromatic substituent, whereas the planar benzene ring (**13**) and the bulkier (benzotriazol-1/2-yl)methyl residue (**15–18**) yielded a negative outcome, abolishing completely the activity. It is worth noting that the topology of the benzotriazole moiety, when combined with the favorable 2-benzyl and dialkyaminoethyl substitutions, also has a prevalent negative impact on the activity, *i.e.* abolishing it.

The substituent in positions 3 and/or 4 of the benzyl ring did not play a significant role in the interaction with the molecular target, since both the unsubstituted derivative (**2**) and those functionalized with electron-withdrawing (**4**, **11**) and electron-donor groups (**1**, **3**, **8**) were tolerated. Indeed, the nature of the substituents on the benzyl ring dictated the agonist/antagonist behavior: in fact, the replacement of the 4-ethoxy group (**3**) with the 3,4-diCl substitution (**11**) on the benzyl ring changed the agonist ability to the antagonist/inverse agonist one. Thus, the 4-ethoxy (or 4-methoxy) benzyl moiety was confirmed to be the main feature for the agonist activity, as well as of this class of benzimidazoles. Moreover, the here presented full agonist activity of compound **3** matches with its analgesic properties (and those of analogs **1**,

Table 1 Binding assays[a] on CB_1 and CB_2 receptors of benzimidazoles **1–18**

Cpd	CB1 K_i (μM)	Max tested conc. on CB1[b] (μM)	CB2 K_i (μM)	Max tested conc. on CB2[b] (μM)	SI (CB1 K_i/CB2 K_i)
1	>10	10 (3.23 ± 1.49)	2.07 ± 0.86	50 (83.69 ± 0.55)	>4.83
2	>10	10 (19.64%)	1.58 ± 0.21	50 (81.73%)	>6.33
3	>10	10 (13.81%)	0.42 ± 0.09	25 (94.11%)	>23.81
4	>10	10 (10.47%)	0.98 ± 0.05	25 (92.69%)	>10.20
5	>10	10 (19.25%)	>10	10 (16.79%)	—
6	>10	10 (5.50%)	>10	10 (19.68%)	—
7	>10	10 (24.29%)	>10	10 (38.47%)	—
8	>10	10 (25.52%)	0.96 ± 0.16	25 (90.40%)	>10.42
9	>10	10 (47.62%)	>10	10 (15.56%)	—
10	>10	10 (37.86%)	>10	10 (48.30%)	—
11	~10	10 (53.94%)	0.37 ± 0.08	10 (94.26%)	27.03
12	>10	10 (41.40%)	~10	10 (53.77%)	>1
13	>10	10 (1.95%)	>10	10 (46.94%)	—
14	>10	10 (5.58%)	>10	10 (24.15%)	—
15	>10	10 (19.03 ± 13.06)	>10	10 (17.29 ± 6.41)	—
16	>10	10 (14.07 ± 0.72)	>10	10 (24.57 ± 3.13)	—
17	>10	10 (15.00 ± 13.01)	>10	10 (17.49 ± 10.97)	—
18	>10	10 (17.63 ± 8.01)	>10	10 (10.13 ± 12.08)	—

[a] Data are the means ± SEM of at least n = 3 experiments. [b] % of displacement.

8) we previously found in *in vivo* studies[18a] and with the relevant role of CB2 agonists in controlling pain.[31]

Concerning the influence of substituents in position 5 in the active 2-benzylbenzimidazole set, the lipophilic electron-withdrawing CF_3 group (**1–4**), compared to the acetyl one (**8**), allowed higher K_i values towards the CB2 receptor to be reached, also generating a greater number of active compounds (ratio 5 : 1). Finally, the chemical variation of the H-bond acceptor acetyl group, as for the CB2 ligand **8**, with the H-bond donor hydrazone group (**14**) was however detrimental to the activity, leading to the loss of affinity for the CB2 receptor.

Functional activity at CB2 receptors

Based on the results obtained, we further evaluated the capability of compounds **3** and **11** to activate CB2 receptors. We used the cAMP Hunter™ assay enzyme fragment complementation chemiluminescence detection kit (Eurofins DiscoverX Corporation, Fremont, CA) to measure whether the compounds modulate intracellular cAMP levels in NKH-477-stimulated CHO cells overexpressing human CB2 receptors. As shown in Fig. 5, compound **3** displayed typical orthosteric G_i agonist behavior by reducing cAMP levels induced by NKH-477 (a water-soluble analog of forskolin). Compound **11** slightly increased the cAMP levels compared to that induced by NKH-477 (Fig. 5A). However, when tested in the presence of an EC_{80} CB2-ligand challenge (3 μM JWH-133), this compound was able to displace the agonist, increasing the level of cAMP up to the NKH-477 stimulus as expected for an orthosteric antagonist/inverse agonist (Fig. 5B).

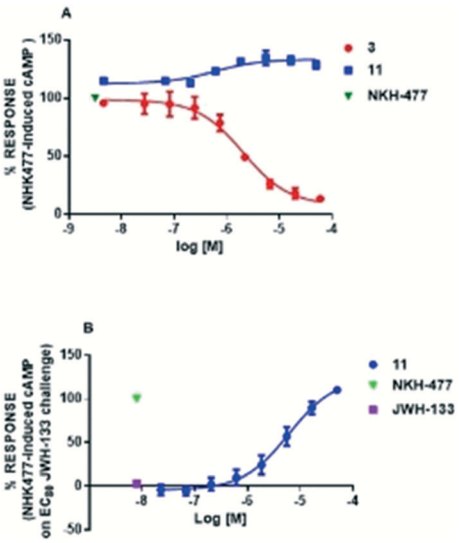

Fig. 5 Concentration–response curves of compounds **3** and **11** measured using the cAMP Hunter™ assay enzyme fragment complementation chemiluminescence detection kit. (A) Effect of increasing concentrations of compounds on NKH-477-induced cAMP levels. (B) Effect of compound on the stimulus of NKH-477 in the presence of a challenge of known agonist (3 μM JWH-133).

Molecular docking studies

In this work, we deepened our study by performing molecular docking calculations focused on the most promising benzimidazoles here investigated (**1–4**, **8** and **11**, Fig. 4) and on the reference compounds **2b**, **3b** and **5b** (Fig. 3). In particular, we wanted to explore the role played by some key decorations on this chemotype at the CB2 receptor binding cavity, by means of the in-house homology model of the human CB2 receptor.[24] This model was built in the presence of the reference agonist WIN-55,212-2 and refined by molecular dynamics simulations (MD), in order to better clarify the interacting role played by the biological target when coupled with the related agonist. Briefly, the derived model displayed a CB2 agonist recognition site delimited by TM3, TM5 and TM6, which was in agreement with site-directed mutagenesis data and other computational studies from the literature.[32]

Our previous MD results revealed a molecular portrait in which the agonist WIN-55,212-2 is bound with a high conformational stability at the receptor binding site, being H-bonded to S112, N188 and S285. In addition, a number of hydrophobic interactions keep the molecule strictly associated with the protein.[24] According to our calculations, the agonist prototypes by AstraZeneca namely **2b** and **3b** oriented the carboxamide function towards the receptor cavity delimited by L108, S112 and F117 (Fig. 6).

As we previously reported for WIN-55,212-2, this docking mode supported for one the H-bond between the oxygen atom of the two agonists, the carbonyl group and the S112 side-chain. The hydrophobic group linked at position 1 of the benzimidazole core was projected towards S180 and F183 while the phenoxy moiety displayed π–π stacking and cation–π contacts with H94 and F95.

The introduction of rigid and bulkier groups than the ethoxybenzyl ring at position 2 of the benzimidazole, as shown by the inverse agonist **5b**, caused a different positioning of the ligand within the receptor crevice. As a consequence, one nitrogen atom of the benzimidazole was H-bonded to S112 while the aliphatic substituent in position

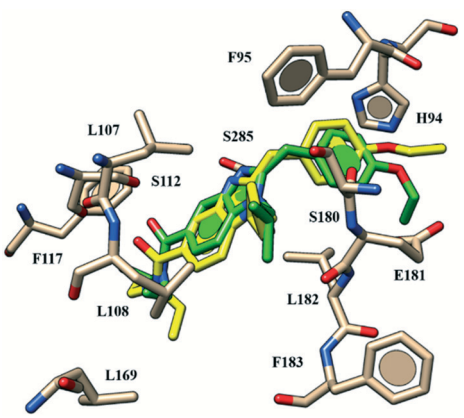

Fig. 6 Docking mode of agonists **2b** (C atom, green) and **3b** (C atom, yellow) within the homology model of the human CB2 receptor.

1 was involved in van der Waals contacts with F95 (Fig. 7). Along with this, the oxygen atom of the substituent placed in position 2 of the benzimidazole displayed one H-bond with the backbone of F183.

All these results suggested a key role determined by those interactions involving S112 for CB2 targeting, while the potency profile especially for the agonist compounds was proved to be increased by means of additional contacts with the aforementioned H94 and F95.

Our compounds **1–18** exhibited only a partially comparable docking mode with agonist and inverse agonist prototypes, sometimes displaying one H-bond between the benzimidazole scaffold and the S112 side-chain (Table 1S†). Notably, this kind of positioning proved to be allowed only in the presence of a small flexible substituent linked at position 1 of the heterocycle, such as the *n*-butyl chain of the inverse agonist compound **11**. These results are in agreement with the lower affinity values featured by the bulkier analogues **15–18**, which are decorated with 2-(benzotriazol-1/2-yl)methyl moieties.

As shown in Fig. 8, the benzimidazole core of **11** should be arranged within the narrow lipophilic cavity delimited by L107, L108 and L169, by detecting van der Waals contacts, as well as moving the aliphatic chain towards F183. This kind of behavior was highly comparable with that discussed for the inverse agonist **5b**, lacking in the H-bond with F183. Conceivably, this caused the lower affinity observed between the two compounds.

On the other hand, the agonist compound **3** was H-bonded to F183 and S285 by the benzimidazole nitrogen atoms and the protonated basic chain, respectively. As reported in Fig. 8, the phenoxy moiety of the agonist only partially mimics the docking mode proposed for the reference compound **2b**.

As a consequence, it should be noticed that the introduction of basic features tethering the N1 nitrogen atom of the benzimidazole ring was not mandatory to afford ameliorated binding affinity values towards CB2, as previously mentioned

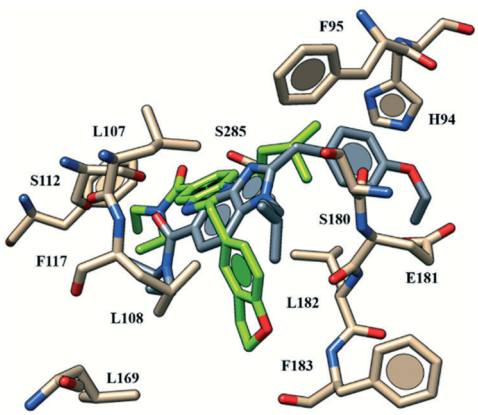

Fig. 7 Docking mode of agonist **2b** (C atom, gray) and inverse agonist **5b** (C atom, green) within the homology model of the human CB2 receptor.

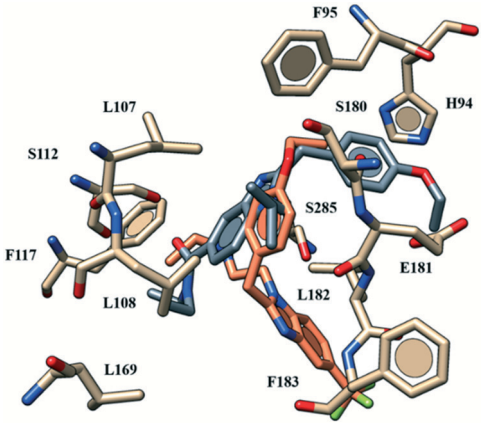

Fig. 8 Docking mode of agonist **2b** (C atom, gray) and benzimidazole **3** (C atom, coral) within the homology model of the human CB2 receptor.

for some series of CB2 indole-containing ligands. Along with this, compound **11** and the related basic analogue **4** displayed comparable K_i values. The quest for gaining more H-bonds with the aforementioned residue was explored with preliminary substitutions linked to N1, bearing ether moieties such as the methyl ethyl ether function exhibited by **12**. This benzimidazole derivative was endowed with a modest CB2 binding ability, supporting further elongation strategies to be applied at this position of the scaffold, by means of suitable H-bonding features.

Prediction of ADMET properties

In the search for novel and more druggable compounds, the *in silico* prediction of descriptors related to absorption, distribution, metabolism, excretion and toxicity (ADMET) properties allows efficient prioritization of the most promising chemical entities to be further developed.[33–35]

In this work, for the most promising benzimidazoles proposed as CB2 ligands (**1–4**, **8**, **11**), a series of ADMET properties were calculated. In detail, we took into account the logarithmic ratio of the octanol–water partitioning coefficient (clog *P*), extent of blood–brain barrier permeation (log BB), rate of passive diffusion-permeability (log PS), human intestinal absorption (HIA), volume of distribution (V_d), the role played by plasmatic protein binding (% PPB) and by the compound affinity toward human serum albumin ($\log K_{aHSA}$), and an overall perspective of the molecule oral bioavailability (% *F*). In addition, preliminary data concerning metabolism and toxicity profiles of any compound were predicted, in terms of the ability to behave as a cytochrome P450 3A4 inhibitor or a substrate and calculating the median lethal dose (LD_{50}) by oral administration.

As shown in Table 2, all the compounds apart from **11** were predicted to weakly pass the central nervous system, being characterized by adequate lipophilicity values (calculated cLog *P* around 5). Notably, these derivatives exhibited favourable volume of distribution values (V_d) and suitable

Table 2 Calculated ADMET descriptors related to absorption and distribution properties

Cpd	clog *P*	log BB[a]	log PS[b]	HIA[c] (%)	V_d[d] (L kg^{-1})	% PPB	log K_{aHSA}	% *F* (oral)
1	5.58	0.47	−1.4	100	8.0	97.98	4.60	99.3
2	5.31	0.40	−1.3	100	8.1	98.12	4.60	99.3
3	5.96	0.48	−1.6	100	9.2	98.11	4.62	99.3
4	5.65	0.41	−1.4	100	7.7	99.01	5.28	97.6
8	4.53	0.59	−1.4	100	5.7	94.75	4.55	99.1
11	6.86	−0.11	−1.3	100	5.3	99.61	5.61	19.9
12	5.99	−0.03	−1.1	100	3.5	99.51	5.56	14.2

[a] Extent of brain penetration based on the ratio of total drug concentrations in tissue and plasma under steady-state conditions. [b] Rate of passive diffusion-permeability. PS represents the permeability–surface area product and is derived from the kinetic equation of capillary transport. [c] HIA represents the human intestinal absorption, expressed as the percentage of the molecule able to pass through the intestinal membrane. [d] Prediction of volume of distribution (V_d) of the compound in the body.

bioavailability profiles (% *F*). Conversely, **11** was ineffective in brain permeability, featuring a too high lipophilicity profile and low bioavailability values. All the analysed derivatives are fully adsorbed at the human intestinal membrane (HIA). None of the compounds here proposed should be involved in cytochrome P450 3A4 inhibition events (Table 2), as all of them are substrates for the same enzyme. Finally, all the derivatives exhibited an acceptable toxicity profile, with the estimated LD_{50} being in the range of 690–1100 mg kg^{-1} for mouse, after oral administration. Accordingly, compounds **11** and **12**, previously tested in antiviral assays (mean EC_{50} = 10 μM on CVB-5 and RSV viruses), didn't show any toxic effect ($CC_{50} > 100$ μM) both against the human MT-4 and primate Vero 76 cell lines.[21]

Conclusions

We developed a series of novel CB2 receptor ligands featuring a benzimidazole core, which is again confirmed to be a valuable scaffold capable of efficient interaction with cannabinoid receptors. The influence on CB2 affinity of some structural features was analyzed, taking into account the information derived from our previous computational studies on the CB2 receptor model,[24] which demonstrated the validity of incorporating small flexible substituents in position 1, a benzyl moiety in position 2 and lipophilic groups (*i.e.* CF_3) in position 5 as suitable decorations of the benzimidazole framework for promoting CB2 binding affinity. In fact, 1-(2-diethylaminoethyl)-2-(4-ethoxybenzyl)-5-trifluoromethylbenzimidazole (**3**) and 1-butyl-2-(3,4-dichlorobenzyl)-5-trifluoromethylbenzimidazole (**11**) proved to be the best promising ligands providing sub-micromolar K_i values and greater preference towards the CB2 receptor. Interestingly, the present study allowed the identification of the agonist ability of compound **3**, which might be correlated with the previously described analgesic activity of this compound, and the inverse agonist/antagonist profile of compound **11**, as a consequence of a simple but significant chemical variation of substituents on the benzyl ring.

Docking studies were performed to study whether the active compounds could target the CB2 receptor, revealing the key contacts for further assessment. From this information, the 2-benzyl-5-trifluoromethylbenzimidazole derivative (**12**), bearing an ethereal function in the 1-(2-methoxy)ethyl chain, although being less effective than compounds **3** and **11**, could also represent an interesting prototype to explore new side chains, more appropriately decorated by means of H-bonding features, capable of gaining interactions with the N188 residue of the CB2 receptor cavity.

The preliminary information concerning their pharmacokinetic profile points to a prevalent peripherally-restricted activity devoid of toxicity that, in combination with the previously found analgesic (not related to opioid receptors) and anti-inflammatory activities, suggests the eventual involvement of CB2 response for explaining their potential biological application.

The results obtained in this study allowed the identification of interesting benzimidazole-containing hit compounds, worthy of further investigation towards even more potent and selective CB2 ligands.

Experimental

Chemistry

Chemicals, solvents and reagents used for the syntheses were purchased from Sigma-Aldrich or Alfa Aesar, and were used without any further purification. Column chromatography (CC): neutral alumina (Al_2O_3), activity 1 (Merck). Mps: Büchi apparatus, uncorrected. ^{1}H NMR and ^{13}C NMR spectra: Varian Gemini-200 spectrometer; $CDCl_3$; δ in ppm rel. to Me4Si as the internal standard. *J* in Hz. Elemental analyses were performed on a Carlo Erba EA-1110 CHNS-O instrument in the Microanalysis Laboratory of the Department of Pharmacy of Genoa University.

1-[2-(Diethylamino)ethyl]-2-(4-ethoxybenzyl)-5-(1-hydrazono ethyl)-1*H*-benzimidazole (14)

To a solution of 5-acetyl-1-[2-(*N*′,*N*′-diethylamino)ethyl]-2-(4-ethoxybenzyl)-1*H*-benzimidazole (compound **8**, 0.38 mmol) in EtOH, a solution of hydrazine hydrate (0.44 mmol) in 3 mL of H_2O was added and then refluxed for 5 h with stirring. At r.t., 5 mL of H_2O was added to the reaction mixture, which was allowed to stand at cooling (0–5 °C) for 12 h. A pale

brown solid was collected by filtration and re-crystallized with dry Et_2O.

Pale brown crystals; yield: 47%. mp: 80–82 °C (Et_2O an.); ^{1}H NMR (200 MHz, $CDCl_3$): δ = 0.94 (t, J = 6.8, 6H, $N(CH_2CH_3)_2$), 1.39 (t, J = 6.8, 3H, OCH_2CH_3), 2.23 (s, 3H, $CH_3C{=}N{-}NH_2$), 2.31–2.63 (m, 6H, $CH_2CH_2N(CH_2CH_3)_2$), 3.83 (m, 2H of $CH_2CH_2N(CH_2CH_3)_2$ and 2H of OCH_2CH_3); 4.31 (s, 2H, CH_2–Ar), 5.05 (br. s, 2H, NH_2, exchange with D_2O), 6.83 (d, J = 7.4, 2 arom. H), 7.16 (d, J = 7.6, 2 arom. H), 7.27 (d, J = 8.6, 1 arom. H), 7.72 (d, J = 8.8, 1 arom. H), 7.93 (s, 1 arom. H); ^{13}C NMR (50 MHz, $CDCl_3$): δ = 156.90, 153.21, 147.36, 141.51, 134.24, 132.90, 128.41, 127.19, 119.31, 115.88, 113.79, 108.1, 90.53, 62.41, 50.80, 46.47, 41.96, 32.59, 13.75, 11.07, 10.66; anal. calcd for $C_{24}H_{33}N_5O$: C 70.73, H 8.16, N 17.18, found: C 70.67, H 8.47, N 17.43.

Molecular modeling

All the compound isomers were built, parameterised (Gasteiger–Huckel method) and energy minimised within MOE using the MMFF94 force field.[36] Docking studies were performed using the available in-house complex of the homology CB2 receptor model in the presence of the reference agonist WIN-55,212-2, whose construction details were reported in our previous publications.[24] Molecular docking calculations were conducted by means of the LeadIT 2.1.8 software suite (www.biosolveit.com). This tool includes the FlexX scoring algorithm, which is based on the calculation of the binding free energy by means of the Gibbs–Helmholtz equation.[37–39] The software detects the binding site defining a radius of 10 Å far from the ligand place in the binding site, in order to set up a spherical search space for the docking approach. The standard setting as the docking strategy was followed, choosing the so-called hybrid approach (enthalpy and entropy criteria); the related scoring function evaluation is described in the literature.[40] The ten derived docking poses were prioritized taking into account the score values of the lowest energy pose of the compounds docked to the protein structure. All the ligands were further refined and rescored by assessment with the algorithm HYDE, included in the LeadIT 2.1.8 software. The HYDE module considers dehydration enthalpy and hydrogen bonding.[41,42] Then, the stability of the selected protein–ligand complexes was verified using a short ~1 ps run of molecular dynamics (MD) simulation at constant temperature, followed by an all-atom energy minimization (LowModeMD implemented in MOE software). In this way, we performed an exhaustive conformational analysis of the ligand receptor binding site subset, as we previously reported for other case studies.[34,43,44]

In silico evaluation of pharmacokinetic properties

The prediction of ADMET properties was performed using the Advanced Chemistry Development (ACD) Percepta platform (www.acdlabs.com). Any ADMET descriptor was evaluated by Percepta using training libraries implemented in the software, which include a consistent pool of molecules with experimentally known pharmacokinetic and toxicity profiles.

Binding assays

Membranes from HEK-293 cells stably transfected with the human recombinant CB1 receptor (B_{max} = 2.5 pmol mg^{-1} protein) and human recombinant CB2 receptor (B_{max} = 4.7 pmol mg^{-1} protein) were incubated with [^{3}H]-CP-55940 (0.14 nM/K_d = 0.18 nM and 0.084 nM/K_d = 0.31 nM, respectively, for CB1 and CB2 receptors) as the high affinity ligand and displaced with 10 μM WIN 55212-2 as the heterologous competitor for non-specific binding (K_i values of 9.2 nM and 2.1 nM, respectively, for CB1 and CB2 receptors). All the compounds were tested following the procedure described by the manufacturer (Perkin Elmer, Italy). Displacement curves were generated by incubating drugs with [^{3}H]-CP-55,940 for 90 minutes at 30 °C. K_i values were calculated by applying the Cheng–Prusoff equation to the IC_{50} values (obtained by GraphPad) for the displacement of the bound radioligand by increasing the concentration of the test compound. Data are means ± SEM of at least n = 3 independent experiments.

Functional activity at CB2 receptors

We used the cAMP Hunter™ assay enzyme fragment complementation chemiluminescence detection kit to characterize the functional activity in a CB2 receptor-overexpressing cell line. Gi-coupled cAMP modulation was measured following the manufacturer's protocol (DiscoveRx, Fremont, CA) as previously reported.[45] Briefly, the cells were incubated for 30 min at 37 °C with the samples prepared in the presence of the cell assay buffer containing 25 μM NKH-477 (a water-soluble analogue of forskolin) to stimulate adenylate cyclase and enhance basal cAMP levels. For compound **11**, the cells were pre-incubated with increasing concentration of the sample, and incubated with the agonist challenge (JWH-133) at its EC_{80} concentration (3 μM, previously determined in separate experiments) in the presence of NKH-477. Luminescence was measured using a GloMax Multi Detection System (Promega, Italy). Data are normalized to the maximal and minimal responses observed, and are reported as mean ± SEM of three independent experiments conducted in triplicate. Data analysis was done using PRISM software (GraphPad Software Inc, San Diego, CA).

Author contributions

MT and EC conceived the study; MT and BT designed and synthesized all the molecules and provided their structural characterization; EC performed the computational studies; AL and AR performed the binding experiments; AM performed the functional assays; MT, EC, PF and AL analyzed and discussed the results; MT and EC wrote the manuscript.

Conflicts of interest

There are no conflicts to declare.

Acknowledgements

This work was financially supported by the University of Genoa, Italy. The authors would like to thank Mr. V. Ruocco for the informatics support to calculations and Mr. O. Gagliardo for performing the elemental analysis. The experiments performed by Alì M. Mahmoud are part of his INCIPIT PhD programme, which is co-funded by the COFUND scheme Marie Skłodowska-Curie Actions.

References

1 R. Kaur, S. R. Ambwani and S. Singh, *Curr. Clin. Pharmacol.*, 2016, **11**, 110–117.
2 A. Ligresti, L. De Petrocellis and V. Di Marzo, *Physiol. Rev.*, 2016, **96**, 1593–1659.
3 A. C. Howlett, F. Barth, T. I. Bonner, G. Cabral, P. Casellas, W. A. Devane, C. C. Felder, M. Herkenham, K. Mackie, B. R. Martin, R. Mechoulam and R. G. Pertwee, *Pharmacol. Rev.*, 2002, **54**, 161–202.
4 S. S.-J. Hu and K. Mackie, *Handb. Exp. Pharmacol.*, 2015, **231**, 59–93.
5 I. B. Adams and B. R. Martin, *Addiction*, 1996, **91**, 1585–1614.
6 D. Piomelli, A. Giuffrida, A. Calignano and F. Rodríguez de Fonseca, *Trends Pharmacol. Sci.*, 2000, **21**, 218–224.
7 J. A. López-Moreno, G. González-Cuevas, G. Moreno and M. Navarro, *Addict. Biol.*, 2008, **13**, 160–187.
8 G. Navarro, P. Morales, C. Rodríguez-Cueto, J. Fernández-Ruiz, N. Jagerovic and R. Franco, *Front. Neurosci.*, 2016, **10**, 406.
9 M. D. Van Sickle, M. Duncan, P. J. Kingsley, A. Mouihate, P. Urbani, K. Mackie, N. Stella, A. Makriyannis, D. Piomelli, J. S. Davison, L. J. Marnett, V. Di Marzo, Q. J. Pittman, K. D. Patel and K. A. Sharkey, *Science*, 2005, **310**, 329–332.
10 M. T. Viscomi, S. Oddi, L. Latini, N. Pasquariello, F. Florenzano, G. Bernardi, M. Molinari and M. Maccarrone, *J. Neurosci.*, 2009, **29**, 4564–4570.
11 J. M. Frost, M. J. Dart, K. R. Tietje, T. R. Garrison, G. K. Grayson, A. V. Daza, O. F. El-Kouhen, L. N. Miller, L. Li, B. B. Yao, G. C. Hsieh, M. Pai, C. Z. Zhu, P. Chandran and M. D. Meyer, *J. Med. Chem.*, 2008, **51**, 1904–1912.
12 J. M. Frost, M. J. Dart, K. R. Tietje, T. R. Garrison, G. K. Grayson, A. V. Daza, O. F. El-Kouhen, B. B. Yao, G. C. Hsieh, M. Pai, C. Z. Zhu, P. Chandran and M. D. Meyer, *J. Med. Chem.*, 2010, **53**, 295–315.
13 P. Diaz, J. Xu, F. Astruc-Diaz, H. M. Pan, D. L. Brown and M. Naguib, *J. Med. Chem.*, 2008, **51**, 4932–4947.
14 P. Diaz, S. S. Phatak, J. Xu, F. Astruc-Diaz, C. N. Cavasotto and M. Naguib, *J. Med. Chem.*, 2009, **52**, 433–444.
15 D. Pagé, H. Yang, W. Brown, C. Walpole, M. Fleurent, M. Fyfe, F. Gaudreault and S. St-Onge, *Bioorg. Med. Chem. Lett.*, 2007, **17**, 6183–6187.
16 D. Pagé, E. Balaux, L. Boisvert, Z. Liu, C. Milburn, M. Tremblay, Z. Wei, S. Woo, X. Luo, Y. X. Cheng, H. Yang, S. Srivastava, F. Zhou, W. Brown, M. Tomaszewski, C. Walpole, L. Hodzic, S. St-Onge, C. Godbout, D. Salois and K. Payza, *Bioorg. Med. Chem. Lett.*, 2008, **18**, 3695–3700.
17 D. Pagé, M.-C. Brochu, H. Yang, W. Brown, S. St-Onge, E. Martin and D. Salois, *Lett. Drug Des. Discovery*, 2006, **2**, 298–303.
18 (*a*) F. Sparatore, V. Boido and F. Fanelli, *Farmaco, Ed. Sci.*, 1968, **23**, 344–359; (*b*) G. Paglietti, M. A. Pirisi, M. Loriga, G. E. Grella, F. Sparatore, M. Satta and P. Manca, *Farmaco, Ed. Sci.*, 1988, **43**, 215–226.
19 M. Tonelli, P. Paglietti, V. Boido, F. Sparatore, F. Marongiu, E. Marongiu, P. La Colla and R. Loddo, *Chem. Biodiversity*, 2008, **5**, 2386–2401.
20 M. Tonelli, M. Simone, B. Tasso, F. Novelli, V. Boido, F. Sparatore, G. Paglietti, S. Pricl, G. Giliberti, S. Blois, C. Ibba, G. Sanna, R. Loddo and P. La Colla, *Bioorg. Med. Chem.*, 2010, **18**, 2937–2953.
21 M. Tonelli, F. Novelli, B. Tasso, I. Vazzana, A. Sparatore, V. Boido, F. Sparatore, P. La Colla, G. Sanna, G. Giliberti, B. Busonera, P. Farci, C. Ibba and R. Loddo, *Bioorg. Med. Chem.*, 2014, **22**, 4893–4909.
22 M. Tonelli, B. Tasso, L. Mina, G. Paglietti, V. Boido and F. Sparatore, *Mol. Diversity*, 2013, **17**, 409–419.
23 M. S. Moolten, J. B. Fishman, J. C. Chen and K. R. Carlson, *Life Sci.*, 1993, **52**, PL199–PL203.
24 E. Cichero, A. Ligresti, M. Allarà, V. Di Marzo, Z. Lazzati, P. D'Ursi, A. Marabotti, L. Milanesi, A. Spallarossa, A. Ranise and P. Fossa, *Eur. J. Med. Chem.*, 2011, **46**, 4489–4505.
25 F. Sparatore, V. Boido and F. Fanelli, *Farmaco, Ed. Sci.*, 1968, **23**, 344–352.
26 F. I. Carroll, R. W. Handy, J. A. Kepler and J. A. Gratz, *J. Heterocycl. Chem.*, 1967, **4**, 262–267.
27 G. Paglietti and F. Sparatore, *Farmaco, Ed. Sci.*, 1972, **27**, 333–342.
28 R. L. Shriner and A. H. Land, *J. Org. Chem.*, 1941, **6**, 888–894.
29 E. Cichero, M. Tonelli, F. Novelli, B. Tasso, I. Delogu, R. Loddo, O. Bruno and P. Fossa, *J. Enzyme Inhib. Med. Chem.*, 2017, **32**, 375–402.
30 G. Paglietti, V. Boido and F. Sparatore, *Farmaco, Ed. Sci.*, 1975, **30**, 504–511.
31 S. Han, J. Thatte, D. J. Buzard and R. M. Jones, *J. Med. Chem.*, 2013, **56**, 8224–8256.
32 T. Tuccinardi, P. L. Ferrarini, C. Manera, G. Ortore, G. Saccomanni and A. Martinelli, *J. Med. Chem.*, 2006, **49**, 984–994.
33 H. Waterbeemd and E. Gifford, *Nat. Rev. Drug Discovery*, 2003, **2**, 192–204.
34 M. Tonelli, S. Espinoza, R. R. Gainetdinov and E. Cichero, *Eur. J. Med. Chem.*, 2017, **127**, 781–792.
35 S. Franchini, L. I. Manasieva, C. Sorbi, U. M. Battisti, P. Fossa, E. Cichero, N. Denora, R. M. Iacobazzi, A. Cilia, L. Pirona, S. Ronsisvalle, G. Aricò and L. Brasili, *Eur. J. Med. Chem.*, 2017, **125**, 435–452.
36 *MOE*, Chemical Computing Group Inc., Montreal H3A 2R7 Canada.
37 H. J. Böhm, *J. Comput.-Aided Mol. Des.*, 1992, **6**, 61–78.
38 H. J. Böhm, *J. Comput.-Aided Mol. Des.*, 1994, **8**, 243–256.

39 M. Rarey, B. Kramer, T. Lengauer and G. Klebe, *J. Mol. Biol.*, 1996, **261**, 470–489.
40 L. Bichmann, Y. T. Wang and W. B. Fischer, *Comput. Biol. Chem.*, 2014, **53**, 308–317.
41 I. Reulecke, G. Lange, J. Albrecht, R. Klein and M. Rarey, *ChemMedChem*, 2008, **3**, 885–897.
42 N. Schneider, S. Hindle, G. Lange, R. Klein, J. Albrecht, H. Briem, K. Beyer, H. Claußen, M. Gastreich, C. Lemmen and M. Rarey, *J. Comput.-Aided Mol. Des.*, 2012, **26**, 701–723.
43 M. Tonelli, L. Naesens, S. Gazzarrini, M. Santucci, E. Cichero, B. Tasso, A. Moroni, M. P. Costi and R. Loddo, *Eur. J. Med. Chem.*, 2017, **135**, 467–478.
44 V. Francesconi, L. Giovannini, M. Santucci, E. Cichero, M. P. Costi, L. Naesens, F. Giordanetto and M. Tonelli, *Eur. J. Med. Chem.*, 2018, **155**, 229–243.
45 N. A. Osman, A. Ligresti, C. D. Klein, M. Allarà, A. Rabbito, V. Di Marzo, K. A. Abouzid and A. H. Abadi, *Eur. J. Med. Chem.*, 2016, **122**, 619–634.

